Available online at www.sciencedirect.com
SCIENCE DIRECT®
Journal of Sound and Vibration 293 (2006) 196–212
JOURNAL OF SOUND AND VIBRATION
www.elsevier.com/locate/jsvi

An advanced direct time domain BEM for 3-D wave propagation in acoustic media

D.C. Rizos*, S. Zhou

Department of Civil and Environmental Engineering, 300 Main St., University of South Carolina, Columbia, SC 29208, USA

Received 17 June 2005; received in revised form 24 August 2005; accepted 28 September 2005
Available online 15 December 2005

Abstract

This paper presents a new Boundary Element Method (BEM) in the direct time domain for the solution of the wave propagation problem in 3D homogenous inviscid acoustic media. The methodology is based on impulse response techniques. To this end, the fundamental solutions associated with the Boundary Integral Equation are derived for concentrated sources of higher order B-spline time modulation. High order spatial discretization is adopted. The solution is obtained in two major steps. First the B-spline Impulse Response Functions (BIRF) for a system of a specific geometry are calculated. BIRF functions are independent of the actual external excitation and need to be calculated only once for a given geometry. The second step calculates the response of the system to arbitrary excitations through a mere superposition of the BIRF functions. This paper discusses the development of the proposed BEM methodology and its validation. The method is shown to be stable regardless of the selection of the analysis time step, as opposed to the retarded potential techniques reported in the literature. The high level of accuracy and the efficiency of the method are demonstrated.

1. Introduction

A class of challenging problems encountered in hydrodynamics pertains to propagation of acoustic waves in infinite or semi-infinite media and the calculation of the transient response of coupled fluid–structure systems. Boundary Element Methods (BEM) have been developed and widely used for wave propagation in elastodynamic or acoustic infinite media because of their ability to implicitly satisfy the boundary condition at infinity [1]. They can be classified, in general, into direct time domain (DTD-BEM) and transform domain (TRD-BEM) methodologies. The TRD-BEM methodologies express the governing equation, and obtain solutions, in a TRD through Fourier or Laplace transformation techniques. DTD-BEM formulations obtain time histories of the solution directly in time, accommodating direct coupling with other methods, such as the Finite Element Method (FEM), for the analysis of coupled media. DTD-BEM methods for wave propagation in acoustic media find their origin in the retarded potential (RP) formulations implemented first in the 1960s by Mitzner [2] to the problem of transient scattering from a hard surface. The first coupling of RP with the

*Corresponding author. Tel.: +1 803 777 6166; fax: +1 803 777 0670.
E-mail address: rizos@engr.sc.edu (D.C. Rizos).

0022-460X/$ - see front matter © 2005 Elsevier Ltd. All rights reserved.
doi:10.1016/j.jsv.2005.09.018

FEM is reported by Huang and his co-workers [3]. RP formulations have two significant drawbacks [1,4]: (1) The time-dependent response at each step in RP depends on the entire history of the response of the system, making the method non-local in both space and time. As a result the time histories of the response have to be stored at every node of the Boundary Element mesh, making the method inefficient, especially for prolonged excitations. (2) Stability requirements of standard RP formulations are counterintuitive since the time step needs to be greater than a critical value. A number of techniques have been recommended for the stabilization of the method [5,6,12]. However, such techniques do not eliminate the problem but rather provide some control on the convergence of the solution.

In this paper, an advanced time domain BEM formulation is presented for wave propagation in acoustic media. The proposed method uses higher order B-spline fundamental solutions derived for this work. It is developed in the general framework of B-spline impulse response techniques introduced by the author for problems in elastodynamics [7–10]. The proposed methodology addresses both drawbacks of the PR methods. Initial investigations show that the method is highly accurate and always converges for a wide range of the time step selection. The proposed method is very efficient, especially for cases involving multiple loads and prolonged excitations.

The following sections present: (1) a brief statement of the mathematical model; (2) the definition of the B-spline polynomials and the derivation of the B-spline fundamental solutions; (3) the proposed BEM and the concept of the B-spline Impulse Response Function (BIRF); (4) calculation of the system response to arbitrary excitations; (5) discussion of computational aspects; and (6) studies on the accuracy, stability and convergence of the method. In the following formulations indicial notation is adopted, where appropriate, boldface characters indicate matrices or vectors and dots represent derivatives with respect to time.

2. Governing equations and integral representation

The differential governing equation for transient scalar wave propagation in an inviscid, compressible acoustic medium of volume V can be expressed as

$$\nabla^2 p(\mathbf{x},t) - \frac{1}{c^2}\ddot{p}(\mathbf{x},t) + f(\mathbf{x},t) = 0, \tag{1}$$

where p is the velocity potential, $\mathbf{x}$ the position vector, t represents time, f the body source, ∇^2 the Laplacian operator, and c the wave propagation velocity in the medium. Following well-established procedures [1], the differential governing equation can be expressed in a Boundary Integral Equation (BIE) form as

$$c(\boldsymbol{\xi})p(\boldsymbol{\xi},t) = \int_S [G(\mathbf{x},t,\boldsymbol{\xi}|f)q(\mathbf{x},\tau) - T(\mathbf{x},t,\boldsymbol{\xi}|f)p(\mathbf{x},\tau)]\,\mathrm{d}S, \tag{2}$$

where $\mathbf{x}$ and $\boldsymbol{\xi}$ are points in the domain or its boundary, the integration is over the boundary, S, of the domain, and G and T are the associated fundamental solutions. The field variables $p(\mathbf{x},t)$ and $q(\mathbf{x},t) = \partial p(\mathbf{x},t)/\partial \mathbf{n}$ correspond to the potential and its derivative in the direction of the outward normal, $\mathbf{n}$, to the boundary, respectively. The term $c(\boldsymbol{\xi})$ is known as the "jump term" and depends on the location of point $\boldsymbol{\xi}$ and the smoothness of the boundary in its neighborhood.

3. B-spline polynomials and B-spline fundamental solutions

3.1. B-spline polynomials

The B-spline functions are piece-wise smooth polynomials of order k derived on the basis of a knot sequence t_n, $n = 1,\ldots,N$. B-spline polynomials of any order k are generated by the recursive formula:

$$B_n^k(t) = \begin{cases} 1 & t_n < t < t_{n+1}, \\ 0 & \text{elsewhere}, \end{cases} \quad k = 1, \tag{3a}$$

$$B_n^k(t) = \left(\frac{t - t_n}{t_{n+k-1} - t_n}\right) B_n^{k-1}(t) + \left(\frac{t_{n+k} - t}{t_{n+k} - t_{n+1}}\right) B_{n+1}^{k-1}(t), \quad k > 1. \tag{3b}$$

For an equally spaced knot sequence $t_n = n\,\mathrm{d}t$, the B-spline polynomials have two properties that are of prime interest to the proposed methodology:

(1) Any B_n^k polynomial can be expressed by a representative (base) one appropriately shifted in time, i.e.

$$B_n^k(t) = B_0^k(t - n\,\mathrm{d}t). \tag{4}$$

(2) The base polynomial B_0^k is non-zero only within small interval, i.e.

$$B_0^k(t) > 0 \;\; \forall t \in (0, \Delta t), \tag{5}$$

where $\Delta t = k\,\mathrm{d}t$ is known as the B-spline support and depends on the order k. For example, the fourth order ($k = 4$) B-spline polynomial used in this work is expressed as

$$B_0^4(\tau) = \begin{cases} \frac{32}{3}\tau^3, & \tau \in [0, 0.25), \\ -32\tau^3 + 32\tau^2 - 8\tau + \frac{2}{3}, & \tau \in [0.25, 0.5), \\ 32\tau^3 - 64\tau^2 + 40\tau - \frac{22}{3}, & \tau \in [0.5, 0.75), \;\; \tau = \frac{t}{\Delta t}, \\ \frac{32}{3}\tau^3 + 32\tau^2 - 32\tau + \frac{32}{3}, & \tau \in [0.75, 1.0], \\ 0, & \text{elsewhere}, \end{cases} \tag{6}$$

and is shown graphically in Fig. 1. B-spline polynomials are commonly used in function interpolation. Hence, any function $f(t)$ can be represented as a linear combination of B-spline polynomials [10] as

$$f(t) \approx \sum_{i=1}^{j} f(\tau_i) B_0^k(t - t_i), \quad t \in [t_1, t_j], \;\; \tau_i = \frac{t_i + t_{i+1} + \cdots + t_{i+k-1}}{k - 1}, \quad k > 1. \tag{7}$$

Rizos and his coworkers [7,10] employed this function to generate the higher order B-spline fundamental solutions for 3D elastodynamics. The procedures and concepts introduced in that work applies equally in the present formulations.

3.2. B-spline fundamental solutions

A fundamental solution, $G(\mathbf{x}, t; \boldsymbol{\xi}|f)$, is defined as any dynamic state in the domain of interest that satisfies the governing equation, Eq. (1). It corresponds to a point source $f(\mathbf{x}, t) = \delta(\boldsymbol{\xi} - \mathbf{x})g(t)$ applied at point $\mathbf{x}$ (source point) with time modulation $g(t)$. In view of the second derivative appearing in Eq. (1), $g(t)$ has to be at least twice continuously differentiable in time and vanishing for $t < 0$. In view of Eqs. (3)–(6), a cubic B-spline $B_0^4(t)$ polynomial satisfies all the requirements of the time modulation of the point source and is adopted in this

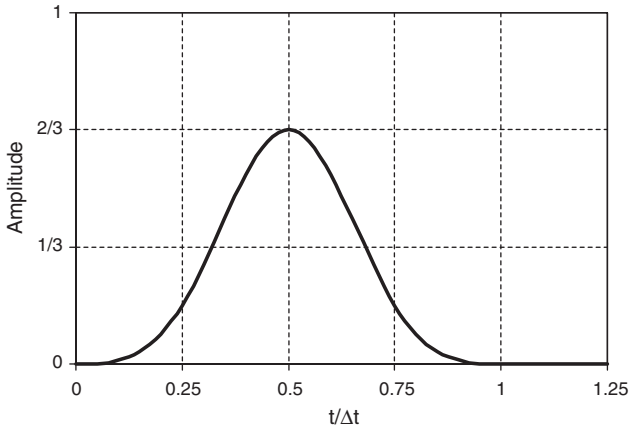

Fig. 1. Graphical representation of cubic B-spline polynomial.

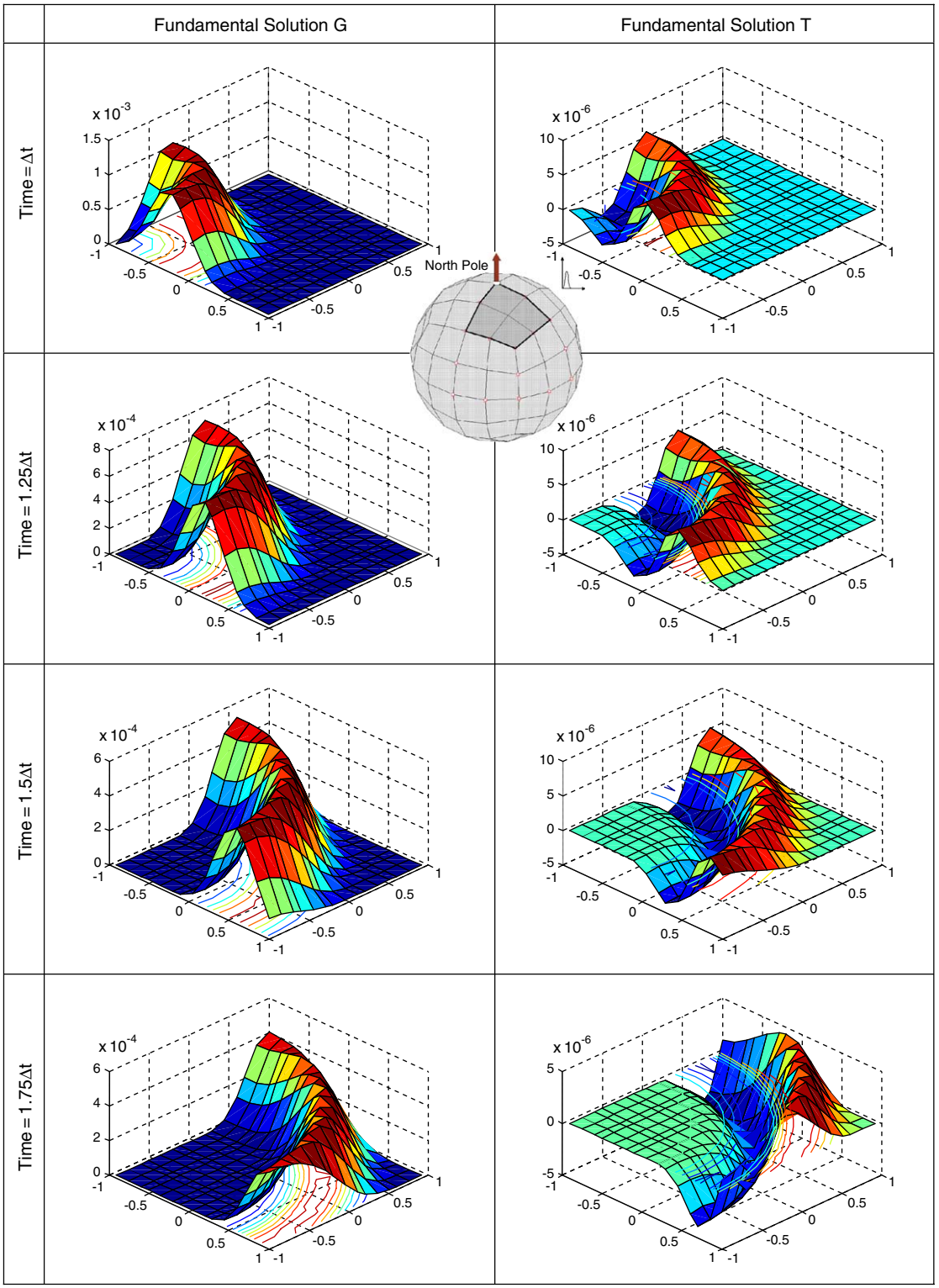

Fig. 2. Graphical representation of B_0^4-spline fundamental solution G and T at selected times.

work for deriving the fundamental solutions which are expressed as

$$G^B = G(\mathbf{x}, t, \xi | \delta(\mathbf{x}-\xi) B_0^4(t)) = \frac{1}{4\pi r} B_0^4\left(\frac{t - r/c}{\Delta t}\right), \tag{8a}$$

$$\begin{aligned} T^B &= T(\mathbf{x}, t, \xi | \delta(\mathbf{x}-\xi) B_0^4(t)) = \frac{\partial G(\mathbf{x}, t, \xi | \delta(\mathbf{x}-\xi) B_0^4(t))}{\partial \mathbf{n}} \\ &= \frac{-1}{4\pi r^2}\left\{ B_0^k\left(\frac{t - r/c}{\Delta t}\right) + \frac{r}{c} \dot{B}_0^k\left(\frac{t - r/c}{\Delta t}\right)\right\} \frac{\partial r}{\partial \mathbf{n}}, \end{aligned} \tag{8b}$$

where $r = |\mathbf{x} - \xi|$ represents the distance between the source point, $\mathbf{x}$, and field points, ξ, over the 3-D solution domain. It is evident that the fundamental solutions are singular when the source point coincides with the receiver point at time t for $0 < t < \Delta t$. Fig. 2 shows the B_0^4-spline fundamental solution for the velocity potential and its normal derivative evaluated at selected times over an element on a surface of a spherical cavity shown in inset of Fig. 2.

4. BEM and the B-spline impulse response function

This section discusses the BEM and the concept of the BIRF associated with the BIE Eq. (2) and the B-spline fundamental solutions, Eqs. (8).

4.1. BIE in a discrete form

Following the procedures established in Refs. [7,10], the bounding surface of the solution domain is discretized into NE number of 8-node quadratic quadrilateral surface elements, for a total of NN boundary nodes. Consequently, the geometry and field variables can be interpolated at any time, t, based on a set of shape functions N_i and corresponding nodal values $(\,)_i$, $i = 1, 2, \ldots, 8$ as

$$\mathbf{x} = N_i \mathbf{x}_i, \quad p(\mathbf{x}, t) = N_i p_i(t), \quad q(\mathbf{x}, t) = N_i q_i(t). \tag{9}$$

Introducing the spatial discretization indicated in Eq. (9), the B-spline fundamental solutions, Eq. (8), and the time knot sequence that defines the B_0^4-spline polynomial of the fundamental solution into the BIE Eq. (2), the latter is written in a discrete form in space and time as

$$\begin{aligned} c(\xi) p(\xi, t^N) = \sum_{n=1}^{N+1} \sum_{\mathrm{el}=1}^{\mathrm{NE}} \Bigg\{ &\int_{S_{\mathrm{el}}} G^B((N_i \mathbf{x}_i), t_n, \xi | B_0^4)(N_i q_i(t_{N-n+2}))\, \mathrm{d}S_{\mathrm{el}} \\ &- \int_{S_{\mathrm{el}}} T^B((N_i \mathbf{x}_i), t_n, \xi | B_0^4)(N_i p_i(t_{N-n+2}))\, \mathrm{d}S_{\mathrm{el}} \Bigg\}, \end{aligned} \tag{10}$$

where the spatial integration is defined over the area, S_{el}, of every element, el, and the summation with respect to $\mathrm{el} = 1, 2, \ldots, \mathrm{NE}$ indicates superposition over all elements. The summation with respect to $n = 1, 2, \ldots, N+1$ pertains to superposition over all time steps up to step $N+1$ and represents a convolution time integral in a discrete form. It should be noted that the proposed method does not require the explicit use of any time integration algorithms. By writing Eq. (10) for every boundary point, ξ, and appropriately collecting the nodal values, the desired algebraic system of equations is derived which can be solved in a time marching scheme. The system of equations is cast in a matrix form at step N as

$$\frac{1}{2}\mathbf{p}^N = \sum_{n=1}^{N+1} \mathbf{G}^N \mathbf{q}^{N-n+2} - \mathbf{T}^N \mathbf{p}^{N-n+2}, \tag{11}$$

where $\mathbf{p}$ and $\mathbf{q}$ are column matrices of size NN containing nodal values of the potential and its normal derivative, respectively, and superscripts indicate the time step at which quantities are evaluated. The coefficient matrices $\mathbf{G}^N$ and $\mathbf{T}^N$ are of size $\mathrm{NN} \times \mathrm{NN}$ and represent the influence of a boundary node on another boundary node, a typical element of which is a scalar value. The integrations involved in the

evaluation of these matrices are performed numerically using the techniques discussed in Ref. [10] and summarized in Section 6.1.

4.2. B-spline impulse response function (BIRF)

The BIRF of the boundary of the acoustic domain is obtained from the solutions of Eq. (11) by applying a unit B-spline impulse excitation, $\mathbf{q}_j$ of duration Δt at a node j only, i.e.

$$\mathbf{q}_j = \mathbf{d}B_0^k(t),\ i,j = 1,\ldots,\mathrm{NN}, \tag{12}$$

where vector $\mathbf{d}$ is defined as $d_i = \delta_{ij}$ with δ_{ij} being the Kronecker delta. Criteria for the selection of the B-spline support are discussed in Section 6.2. In view of the tension free boundary condition on the surface of the domain, the incident excitation field will generate only a scattered potential field. Noting that the B-spline time modulation of the excitation is embedded in the fundamental solutions, Eq. (11) yields the BIRF, $\mathbf{b}_j^N = \mathbf{p}|_{\mathbf{q}_j}$, as

$$\frac{1}{2}\mathbf{b}_j^N = \mathbf{G}^N\mathbf{q}_j - \sum_{n=1}^{N}\mathbf{T}^n\mathbf{b}_j^{N-n+2} = \mathbf{g}_j^N - \mathbf{T}^1\mathbf{b}_j^{N+1} - \mathbf{T}^2\mathbf{b}_j^N - \sum_{n=3}^{N}\mathbf{T}^n\mathbf{b}_j^{N-n+2}, \tag{13}$$

where $\mathbf{g}_j^N$ is the column of matrix $\mathbf{G}$ that corresponds to the "loaded" jth node. The time stepping scheme expressed in Eq. (13) is an implicit one. The corresponding explicit scheme is obtained by interpolating the potential field at time t^N using cubic B-spline polynomials, Eq. (7), i.e.

$$\begin{aligned}\mathbf{b}^N &= B_0^4(0.75)\mathbf{b}^{N-1} + B_0^4(0.5)\mathbf{b}^N + B_0^4(0.25)\mathbf{b}^{N+1} = \frac{1}{6}\mathbf{b}^{N-1} + \frac{2}{3}\mathbf{b}^N + \frac{1}{6}\mathbf{b}^{N+1}\\ &\Rightarrow \mathbf{b}^{N+1} = 2\mathbf{b}^{N+1} - \mathbf{b}^{N-1}.\end{aligned} \tag{14}$$

Substitution of Eq. (14) into Eq. (13) yields the explicit scheme as

$$\mathbf{b}_j^N = \left(\frac{1}{2}\mathbf{I} + 2\mathbf{T}^1 + \mathbf{T}^2\right)^{-1}\left\{\mathbf{g}_j^N - \sum_{n=3}^{N+1}\mathbf{T}^n\mathbf{b}_j^{N-n+2} + \mathbf{T}^1\mathbf{b}_j^{N-1}\right\}, \tag{15}$$

where $\mathbf{I}$ is the identity matrix. Eq. (15) represents the BIRF of the free surface of the acoustic domain due to the application of a single impulse at node j. Thus, the BIRF vectors, $\mathbf{b}_j^N$, can be computed for all nodes $j = 1,2\ldots,\mathrm{NN}$ and collected in a matrix form as

$$\mathbf{B}^N = [\mathbf{b}_1^N, \mathbf{b}_2^N, \ldots, \mathbf{b}_j^N, \ldots, \mathbf{b}_{\mathrm{NN}}^N]. \tag{16}$$

Eq. (16) is the BIRF of the system expressed in a discrete form in space and time. Each element B_{ij} in the matrix represents the impulse response of node i at time step N due to a "unit" excitation applied at node j. This matrix is a characteristic of the system and needs to be computed only once for the specific geometry of the free surface of the solution domain. In the general case, the B-spline impulse response is computed for all nodes of the problem and the impulse response matrix, $\mathbf{B}^N$, is square. In most practical cases, however, the BIRF of the system needs to be computed only for those nodes that are expected to carry a forced excitation during the solution, yielding a rectangular matrix or a square matrix of significantly reduced size. Because of the small, finite duration of the B-spline impulse excitation, and the wave attenuation, the number of time steps N that the BIRF matrices are obtained for, is small compared to the response of the system to general excitations and limited to only a few time steps, as discussed in Section 6.3. Once this characteristic response of the system is known, the system can be analyzed for any arbitrary transient loading, as discussed in the following section.

5. System response to arbitrary excitation

The function interpolation scheme using B-spline polynomials shown in Eq. (7) indicates that if the BIRF of the system is known, then the response to an arbitrary excitation can be computed as a mere superposition of

the BIRFs. To this end, the vector of arbitrary transient external excitations, $\mathbf{q}(t)$, applied at the boundary nodes of the system is first evaluated at the time knots that define the B-spline polynomial as

$$\mathbf{q}(t = t_n) = \mathbf{q}^n. \tag{17}$$

If $\mathbf{p}^N$ represents the unknown response of the dynamic system to the excitation $\mathbf{q}(t)$ at time step t_N, then the superposition of the fourth order BIRF is expressed as

$$\mathbf{p}^N = \sum_{n=1}^{N+1} \mathbf{B}^n \mathbf{q}^{N-n+2}. \tag{18}$$

The proposed approach is very efficient especially when multiple load cases are considered, since the BIRF functions are independent of the external excitation and are typically of shorter duration than the external excitation, as discussed in Section 6.3.

6. Computational aspects

6.1. Integration of BEM kernels

In view of the retarded time, $t - r/c$, and Eq. (5), the fundamental solutions, Eqs. (8), evaluated at time, t, between a reference boundary node j and any point ξ on the element that defines the area of integration are non-zero over only a part of the element. This area can be thought of as the active zone B_{act} of integration, shown in Fig. 3, and is defined as a function of the distance, r, between the two points and time, t, that satisfies the inequality

$$B_{\text{act}}(r, t) \equiv \{r, t : (t - \Delta t)c \leqslant r \leqslant tc\}. \tag{19}$$

The integration of BEM kernels, shown in Eq. (10), requires integration of the B-spline fundamental solutions over the active zone, B_{act}, within a boundary element. Standard Gaussian quadrature applied over the entire element area is inaccurate and the element subdivision techniques introduced in Ref. [10] are adopted in this work for both the singular and non-singular cases. This procedure is based on the division of the parent element into a number of K rectangular subelements each one of area D_k. Each subelement is distinguished by the lengths of its side $\Delta\eta_1^k$ and $\Delta\eta_2^k$ and the coordinates η_1^k, and η_2^k, of its center, as shown in Fig. 3. Gaussian quadrature is applied over each subelement and the surface integrals over a quadrilateral element is computed

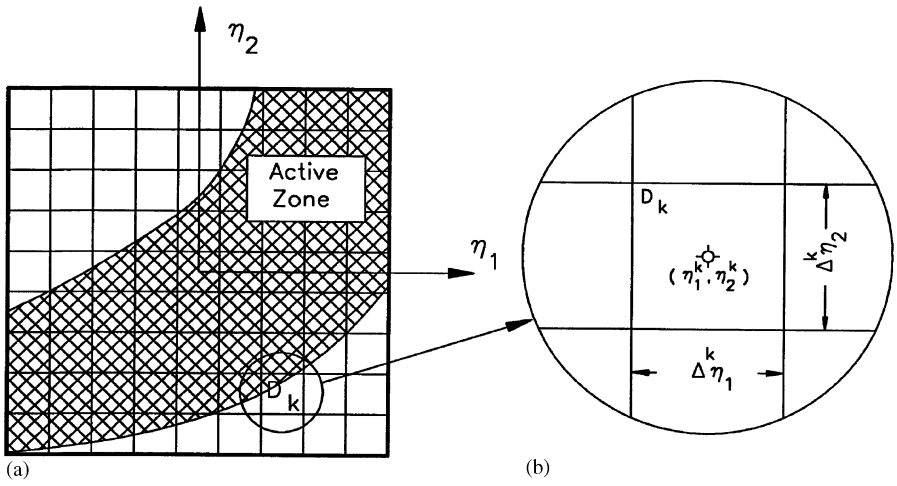

Fig. 3. Definition of active zone and integration subelement on a quadrilateral element (adapted from Ref. [10]): (a) 8-node parent element, (b) subelement D_k.

numerically as

$$\int_{S_{el}} f(x)\,\mathrm{d}B \approx \frac{1}{4}\sum_{k=1}^{K} D_k \sum_{i=1}^{n} n \sum_{j=1} w_i w_j f(\xi_1,\xi_2)|G(\xi_1,\xi_2)|, \tag{20}$$

where $\xi_1 = 0.5\Delta\eta_1^k\psi_i + \eta_1^k$ and $\xi_2 = 0.5\Delta\eta_2^k\psi_i + \eta_2^k$, ψ_i are the abscissas in interval $(-1,1)$, and w_i are the associated weights. Function $f(\eta_1,\eta_2)$ represents the integrands of the form shown in Eq. (10) and $|G(\xi_1,\xi_2)|$ is the Jacobian of transformation. For the singular case, in addition to the element subdivision scheme, the successive coordinate mapping along with triangle coordinates is directly adopted from Ref. [10]. The employment of cubic B-splines in the fundamental solution and the representation of the boundary by quadratic elements yield B-spline fundamental solutions with two continuous derivatives within the active zone. The continuity of the B-spline fundamental solution, in view of the proposed modified quadrature scheme, has the advantage that the required number of subdivisions solely depends on the desired accuracy at which the active zone is modeled.

6.2. Selection of time step and convergence

The selection of the B-spline support, Δt which defines the time step of the solution ($\mathrm{d}t = \Delta t/4$, for cubic B-splines), depends on three factors: (1) the wave velocity of the medium in relation to the maximum extents of the BEM mesh, (2) the wave velocity of the medium in relation to its element size, and (3) the form of the external excitation.

The time required by a wave front to travel between two points in the domain that are the furthest apart is defined as

$$t_0 = \frac{r_{\max}}{c}, \tag{21}$$

where $r_{\max}$ is the distance between the two points. It is noted that if a chosen Δt is close to t_0, the resolution of the time history of the response will be very poor. In fact, if $\Delta t \geqslant 4t_0$, no response will be calculated since in a single time step the waves will "jump over" the entire domain. Therefore, it is recommended to choose a B-spline support so that

$$\Delta t \leqslant \frac{r_{\max}}{2c}. \tag{22}$$

In view of the integration schemes presented in Section 6.1, the width of the active zone within an element as given by Eq. (19) depends on the B-spline support. In fact, the smaller the B-spline support the smaller the width of the active zone. Consequently, a large number of subelements are required for the accurate evaluation of the BEM kernels when a very small Δt is selected, sacrificing, thus, the efficiency of the integrations. It is recommended that the B-spline support is selected so that

$$\Delta t \geqslant \frac{L_{\max}}{3c}, \tag{23}$$

where $L_{\max}$ is the maximum element size. Smaller values of B-spline support may be used, however, the number of subelements may increase prohibitively for acceptable levels of accuracy.

Finally, the B-spline support should be selected so that all anticipated external excitations are accurately interpolated using the B-spline function approximation scheme, Eq. (7). The effects of the time step on the accuracy of the solution are demonstrated in Section 7.3.

6.3. Duration and truncation of BIRF

In theory, the duration of the BIRF function is infinite in general. For all practical purposes, however, the duration of the BIRF can be truncated to a few time steps of the solution, as justified in the following. It is indicated in Eq. (13) that the large amplitude component of the BIRF depends on the duration of the G^B and T^B BEM kernels. The duration of the BEM kernels, in turn, depend on the duration of the B-spline impulse excitation, the speed of the medium and the maximum extents of the discretized boundary. Because of the

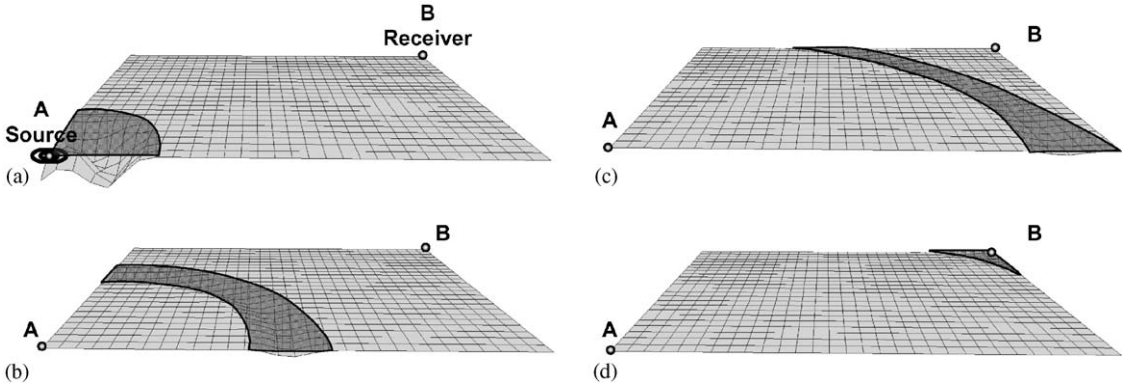

Fig. 4. Propagation of G^B waves on a flat boundary: (a) time step: 4, (b) 11, (c) 19, (d) 25.

small duration of the B-spline impulse used in the fundamental solutions, matrices **G** and **T** are non-zero for an effective time t_{eff} defined as

$$t_{\text{eff}} = \frac{r_{\max}}{c} + \Delta t, \tag{24}$$

where $r_{\max}$ is the distance between the two points on the boundary of the domain that are the furthest apart. This time represents the time required by the last wave front emanated at the source point to travel through, and completely exit, the boundary of the solution domain. For example, in the discretized free surface of a fictitious acoustic medium shown in Fig. 4(a), the distance between two points, A and B, that are the furthest apart is 330 m. The wave velocity is assumed as 600 m/s. When a B-spline impulse of duration $\Delta t = 0.1$ s is applied at point A, the source point, and an analysis time step is considered as $\mathrm{d}t = \Delta t/4$, a zone of wave fronts propagates through the medium, as shown by the shaded areas in Figs. 4(a–d). The G^B and T^B BEM kernels are non-zero for a total of 26 time steps only, representing a $t_{\text{eff}} = 0.65$ s. Furthermore, it should be noted that for the particular example where the boundary of the domain is flat, the T^B BEM kernels is always zero due to the $\partial r/\partial \mathbf{n}$ term appearing in Eq. (8b). Consequently, the duration of the BIRF for this example is also 26 time steps, which is significantly less than the duration of an arbitrary excitation. In the case where the boundary is not flat, the T^B BEM kernels are not zero anymore and the duration of the BIRF function is infinite in theory, as indicated in Eq. (15). This is due to the convolution-like form of the summation in Eq. (15). However, it has been observed that the amplitude of the BIRF decreases rapidly after t_{eff}. This observation is demonstrated in Fig. 5 that depicts a typical BIRF function. It is evident that the large amplitude component lasts approximately t_{eff}. A secondary response of significantly smaller amplitude detected at later times is caused by reflected and refracted waves. Therefore, truncating the duration of BIRF to a few time steps without loss of accuracy is feasible, preserving, thus, the efficiency of the proposed methodology. For all practical purposes it is recommended to truncate the BIRF no sooner than $(1.5)t_{\text{eff}}$. The effects of truncating the BIRF on the solution accuracy are studied in Section 7.4.

6.4. *Efficiency of the proposed method*

It has been reported in the literature that BEM time domain methods are non-local in both space and time, making the methods inefficient especially for prolonged excitations. However, the proposed methodology allows for truncation of the BIRF functions, as discussed in Section 6.3. In general, the duration of the BIRF is significantly less than the duration of an arbitrary excitation. The summation appearing in Eq. (18) for computing the response to arbitrary excitations contains only a few terms corresponding to the non-zero BIRF values. Therefore, although the method is still non-local in time, this represents a significant improvement on the efficiency, especially when the arbitrary excitation may be

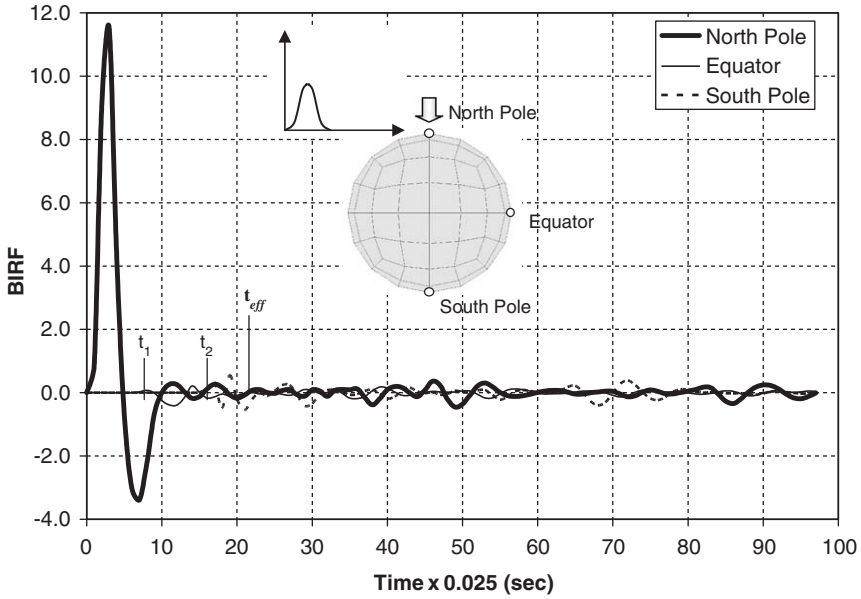

Fig. 5. The BIRF (potential field) of points on the: ▬, "north pole"; —— "equator", and - - -, "south pole", due to excitation (flux) applied at the north pole.

thousands of time steps long. This is especially true when comparing the proposed method with convolution type methods, where the convolution integrals have to be computed at all times of the response for the entire time history.

BEM are known to produce fully populated matrices. However, the coefficient matrices in Eq. (11), and the associated BIRF, Eq. (16), can be extremely sparse due to the nature of the geometric characteristics of the wave fronts generated by the small duration B-spline impulse excitation. For example, Fig. 4(a–d) shows the propagating wave fronts of G^B BEM kernel on a 30×30 mesh of a flat surface. The non-zero entries of matrix G^B correspond to a source point that lies within the shaded areas and any receiver node on the boundary. It is evident that the G^B matrix is sparse since at least 80% of its entries are zero at all times. It should be noted that the smaller the time step the greater the sparsity of the matrices. Similar behavior is observed in BIRF responses. Therefore, although the proposed method is still non-local in space, efficient storage and operation algorithms for sparse matrices can be implemented.

7. Validation studies

This section presents validation studies that demonstrate the accuracy and stability of the proposed methodology. The problem under consideration is a spherical cavity of radius $r_0 = 212\,\text{m}$ submerged in an infinite acoustic medium that is subjected to internal flux. The wave velocity of the acoustic medium is $c = 1000\,\text{m/s}$. This example is treated as a general 3D problem and no advantage is taken of the symmetries of the problem. The surface of the cavity is discretized into 24 8-node quadratic elements for a total of 74 boundary nodes, as shown in the inset of Fig. 5. The BIRF function of the cavity is computed and discussed first. Subsequently, the response of the cavity to harmonic or transient flux is computed and compared to analytic solutions reported in the literature. This section concludes with a study on the effects of the variation of the time step on the convergence of the solution, and the effects of the degree of truncation of the BIRF on the accuracy of the solution.

7.1. B-spline impulse response

In order to calculate the BIRF of the cavity, each of the 74 nodes is exited in turn by a flux $q_i(t) = q_0 B_0^4(t)$, with $q_0 = 1.0$ and the time history of the potential field at all nodes is calculated as discussed in Section 4. The integrations over each element indicated in Eq. (10) are computed based on a 3-point Gaussian quadrature using a 5×5 subelement division. Fig. 5 shows the first 98 steps of the BIRF of the "north pole", a point on the "equator" and the "south pole" for the case where the north pole of the cavity is excited with a B-spline of duration $\Delta t = 0.1$ s. The wave arrival times to the point on the "equator" and "south pole" are indicated by $t_1 = 0.2$ and $t_2 = 0.4$, respectively, representing approximately the theoretical values of $t_1 = 0.212$ and $t_2 = 0.424$ s. The difference is attributed to the coarse discretization. The effective time is computed as $t_{\text{eff}} = 0.524$ s and is also indicated on the graph. It is evident in Fig. 5 that the solution is stable, even at later times.

7.2. Validation with analytic solutions

This section presents validations of the proposed method in the frequency and time domains. For validations in the frequency domain, the spherical cavity is subjected to harmonic flux, $q(\mathbf{x}, t) = q_0 \sin(\omega t)$, of frequency ω and amplitude $q_0 = 1$ m/s that is uniformly distributed on the boundary. An analytic solution for the steady-state response of the potential field, p, at distance r ($r \geqslant r_0$) in the radial direction is reported in Ref. [11] in terms of the wave number $\kappa = \omega/c$. The amplitude of the steady-state response as a function of frequency is obtained in an indirect way using the proposed formulation. To this end, the system is subjected to a series of harmonic excitations with frequencies, ω, in the range 0.5–12.5 rad/s. The time history of the response is calculated in each case as indicated in Eq. (18), using the BIRF obtained in Section 7.1, until a steady-state response has been reached. In each excitation case, the amplitude of the steady-state response is monitored and is shown in Fig. 6(a) as a function of the non-dimensional frequency, $k_a = \omega/cr_0$. Fig. 6(a) also shows the analytic solution [11]. The superior accuracy of the proposed methodology is evident.

For validation in the time domain, the cavity is subjected to a unit amplitude internal flux, $q(\mathbf{x}, t) = 1$, that is uniformly distributed on the boundary. The excitation is suddenly applied and maintained constant throughout the analysis. The analytic solution to this problem has been reported in Ref. [13]. The time history of the potential field is computed by Eq. (18) and the BIRF of Section 7.1 and plotted in Fig. 6(b) for the five different points shown on the surface. A different numerical solution reported in the literature [13] is also shown for comparison. It is evident the proposed method is highly accurate and stable even at later times of the solution.

7.3. Convergence study and effects of time step

This section presents a study on the effects of the B-spline support on the convergence of the solution. To this end, the spherical cavity discussed in Section 7.1 is considered. In this study a non-dimensional B-spline support is defined as

$$\Delta\tau = \frac{\Delta t c}{r_{\max}}, \tag{25}$$

so that a value of $\Delta\tau = 1$ signifies that the time required by a wave to travel through the entire domain is equal to the duration of the excitation B-spline impulse. Seven different B-spline supports are considered, as shown in Table 1. Table 1 also shows the associated time steps and the corresponding non-dimensional values, along with the number of subelements required for the accurate integration of the BEM kernels. The corresponding BIRF functions of the cavity are obtained for the seven B-spline supports listed in Table 1. The cavity is subjected to harmonic excitations of different frequencies, ω, shown in Table 2. The corresponding non-dimensional frequencies, k_a and periods, T, of the harmonic excitations are also listed. The ratio $T/\mathrm{d}t$, shown in Table 2, pertains to the number

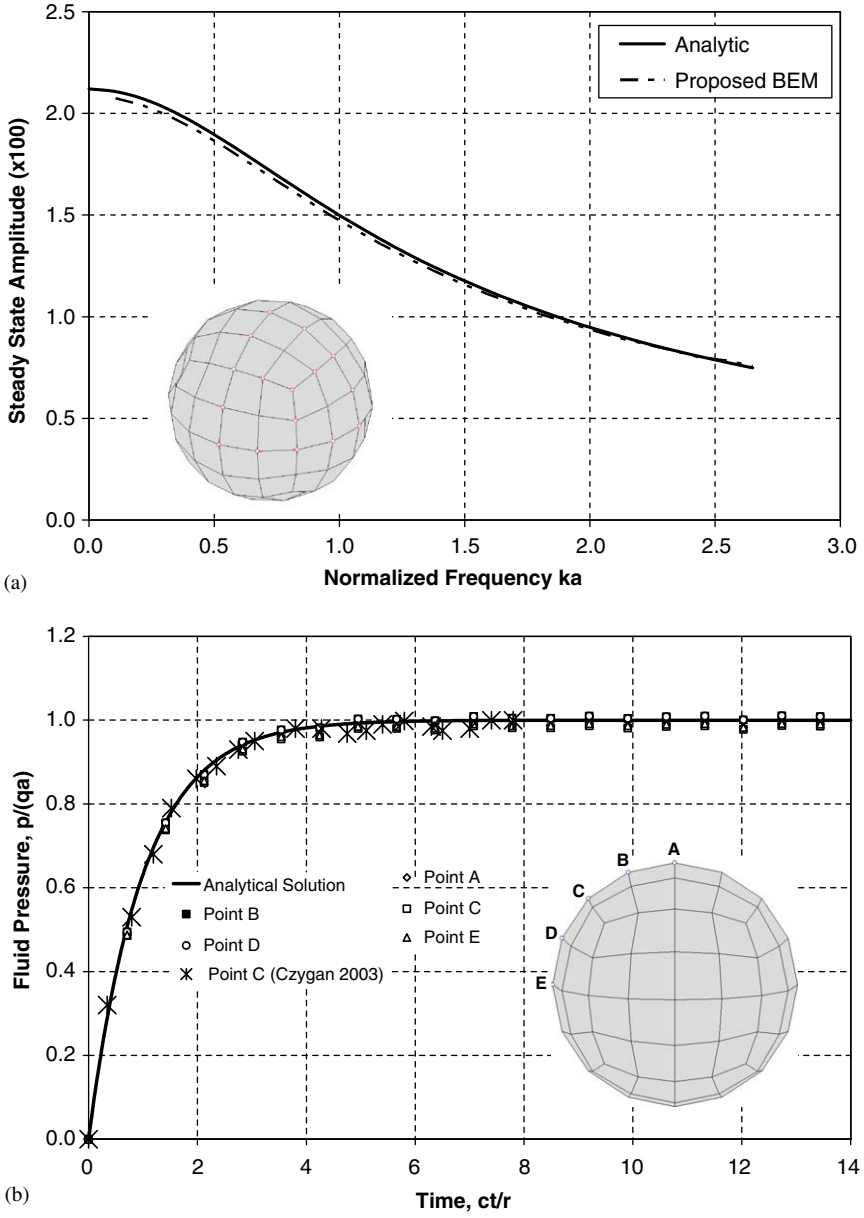

Fig. 6. BEM validation in: (a) frequency domain: ——, analytic; - - -; proposed BEM; (b) time domain: —, analytic; (○), point A; (◇), point B; (■), point C; (□), point D; (△), point E; ✳, point C [13].

of steps that "fit" within a single period and it indicates the quality of the interpolation of the external excitation by B-spline polynomials. In general, the smaller this number, the higher the interpolation error. For each of the excitation frequencies and each B-spline support, the amplitude, A_{BEM}, of the steady-state response is computed and the percentile error with respect to the exact solution, A_{exact}, is determined as

$$E = \frac{A_{\mathrm{exact}} - A_{\mathrm{BEM}}}{A_{\mathrm{exact}}} 100. \tag{26}$$

Table 1
B-spline support, time step, and subelement discretization for convergence studies

Dimensional		Non-dimensional		Subelement discretization
B-spline support Δt	Time step, dt	B-spline support, $\Delta\tau$	Time step, dτ	
0.0125	0.003125	0.0295	0.0074	50×50
0.05	0.0125	0.1179	0.0295	15×15
0.1	0.025	0.2358	0.059	7×7
0.2	0.05	0.4717	0.1179	5×5
0.4	0.1	0.9434	0.2359	5×5
0.6	0.15	1.4151	0.3538	5×5
0.8	0.2	1.8868	0.4717	5×5

Table 2
Frequencies of excitation for convergence studies

ω	k_a	T	$T/\mathrm{d}t$						
			$\mathrm{d}t_1$ 0.00313	$\mathrm{d}t_2$ 0.0125	$\mathrm{d}t_3$ 0.025	$\mathrm{d}t_4$ 0.05	$\mathrm{d}t_5$ 0.1	$\mathrm{d}t_6$ 0.15	$\mathrm{d}t_7$ 0.2
0.5	0.106	12.566	4021.2	1005.3	502.7	251.3	125.7	83.8	62.8
3	0.636	2.094	670.2	167.6	83.8	41.9	20.9	14.0	10.5
6	1.272	1.047	335.1	83.8	41.9	20.9	10.5	7.0	5.2
9	1.908	0.698	223.4	55.9	27.9	14.0	7.0	4.7	3.5
12	2.544	0.524	167.6	41.9	20.9	10.5	5.2	3.5	2.6

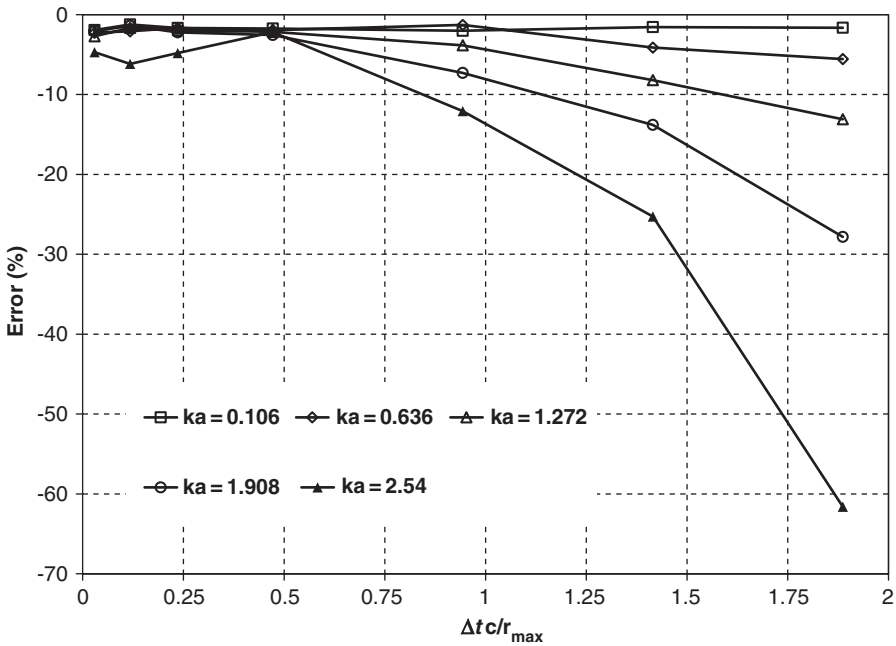

Fig. 7. Effects of B-spline support on solution error: ⊟, $k_a = 0.106$; ◇, $k_a = 0.636$; △, $k_a = 1.272$; ○, $k_a = 1.908$; ▲, $k_a = 2.54$.

The error is plotted as a function of the normalized B-spline support, Eq. (25), and is shown in Fig. 7, for the different frequencies considered. It is observed that:

1. For B-spline support $\Delta t < r_{\max}/2c$, ($\Delta\tau < 0.5$) the solution always converges with an error $< 5\%$.
2. In general, the error increases as the B-spline support increases. This effect is more severe for higher excitation frequencies.
3. The error remains small ($E < 10\%$) for all values of the B-spline support and for low excitation frequencies ($k_a < 1$).

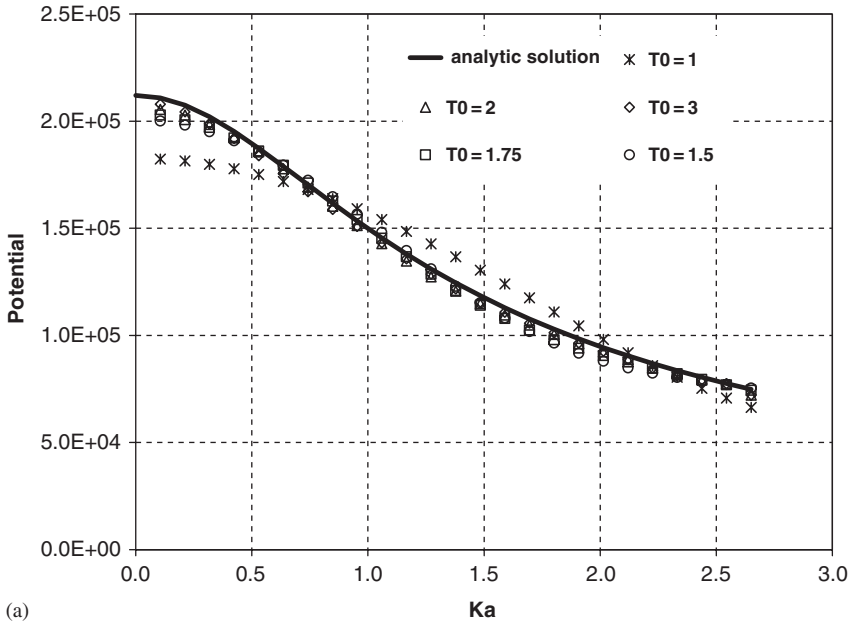

(a)

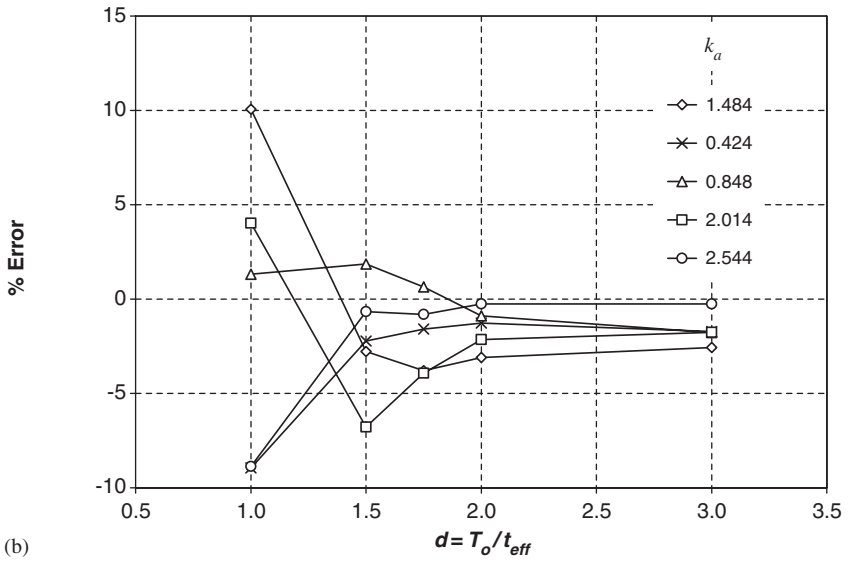

(b)

Fig. 8. Effects of truncation ratio, α, of BIRF on accuracy of solution in frequency domain: (a) frequency plots for: ——, analytic; ✳, $\alpha = 1$; (○), $\alpha = 1.5$; (□), $\alpha = 1.75$; (△), $\alpha = 2$; (◇), $\alpha = 3$; (b) % Error vs. α for frequencies: ✳, $k_a = 0.424$; —△—, $k_a = 0.848$; —◇—, $k_a = 1.484$; —□—, $k_a = 2.014$; —○—, $k_a = 0.2544$.

4. The large error at higher frequencies ($k_a > 1.9$) observed along with a large B-spline support, $\Delta\tau > 1.25$, is attributed rather to the poor interpolation of the excitation, as indicated by the small values of the ratio $T/\mathrm{d}t$ shown in Table 2.

7.4. Efficiency and effects of truncation of BIRF

The duration of the BIRF function may be truncated, as discussed in Section 6.3, contributing, thus, significantly to the efficiency of the method. The effects of truncation on the accuracy of the solution are examined in this section. To this end, the spherical cavity introduced in Section 7.1 is considered. The BIRF of the cavity is based on a B-spline impulse of duration $\Delta t = 0.1$ s, and is computed for a total duration of

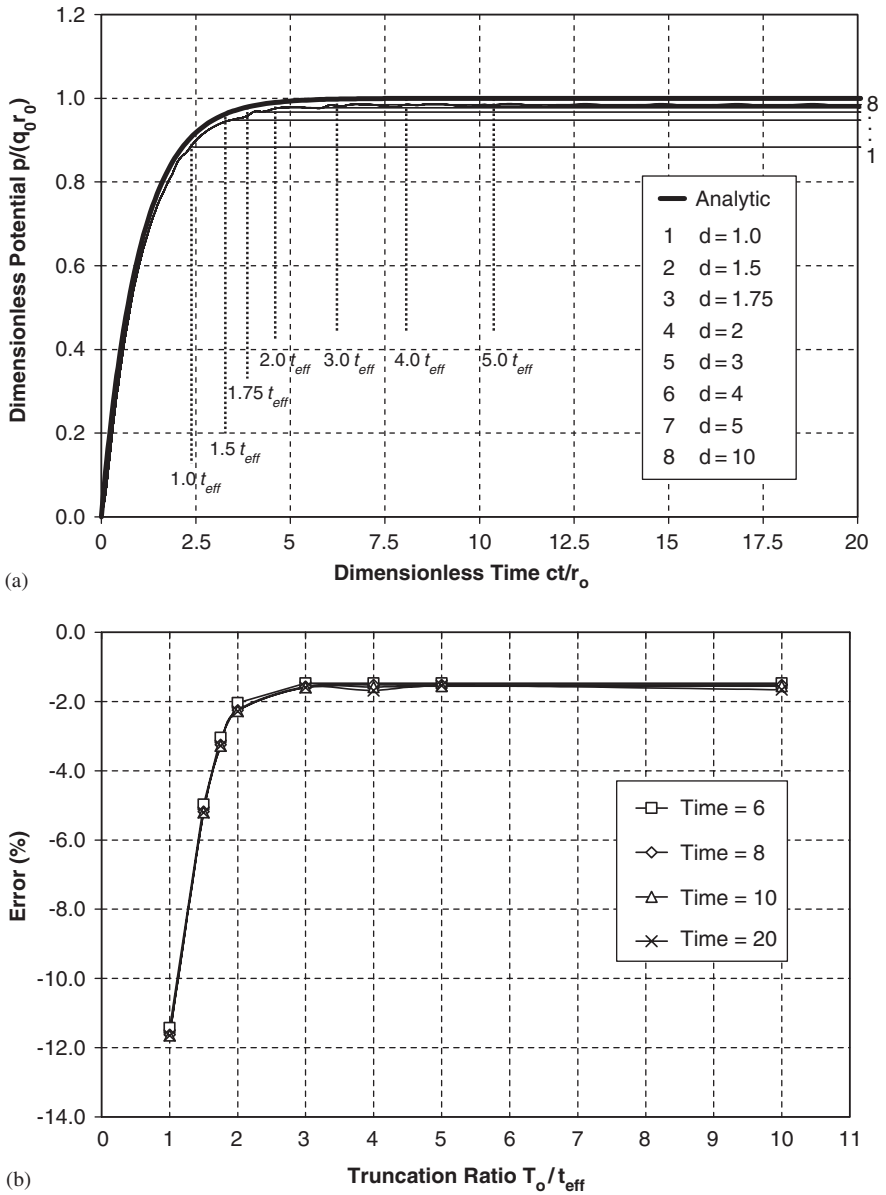

Fig. 9. Effects of truncation ratio, α, of BIRF on accuracy of solution in time domain: (a) time history of radial potential for: ——, analytic; 1, $a = 1$; 2, $a = 1.5$; 3, $a = 1.75$; 4, $a = 2$; 5, $a = 3$; 6, $a = 4$; 7, $a = 5$; 8, $a = 10$. (b) % Error vs. α at selected non-dimensional time: -□-, time = 6; -◇-, time = 8; -△-, time = 10; ✳, time = 20.

$T_{tot} = 5.24$ s, or 210 time steps. It is assumed that the BIRF is zero after T_{tot}. The number of time steps of non-zero BIRF values is important in the efficient implementation of the superposition scheme, Eq. (18), for calculating the response to arbitrary excitations. The selected example is a representative of the general case since the strongly curved surfaces create reflected and refracted waves that appear as oscillations at later times in the BIRF response, as shown in Fig. 5 that shows only the first 98 time steps. The effective time, Eq. (25), for this problem is $t_{eff} = 0.524$ s, or 21 time steps. The truncated duration of the BIRF is considered as $T_0 = \alpha t_{eff}$, where α is a truncation ratio. The present studies are conducted in both the frequency and time domains using the procedures discussed in Section 7.3. However, the duration of the BIRF is truncated for values of the truncation ratio in the range 1–10. Fig. 8(a) shows the frequency plot for different truncation ratios. Fig. 8(b) shows the percentile error, Eq. (26), as a function of the truncation ratio for selected excitation frequencies. In general, it is observed that: (1) even when a severely truncated BIRF ($\alpha = 1$) is used the error does not exceed 15%; (2) for truncation $\alpha = 1.5$ the error is less than 5% for all frequencies, which represents an acceptable accuracy for all practical applications; and (3) for truncations $\alpha > 2.0$ the effects of truncation are negligible. Similar conclusions can be drawn from the time domain studies. The numerical and analytic solutions are plotted in a normalized form in Fig. 9(a). The amplitude of the response is normalized as $p/q_0 r_0$ and the time axis is normalized as ct/r_0. The percentile error with respect to the analytic solution, Eq. (26), is plotted as a function of the truncation ratio for normalized times $ct/r_0 = 6$, 8, 10 and 20. It is observed that: (1) the accuracy at early times, i.e. $t < t_{eff}$, for all truncation ratios is not affected by the truncation itself; (2) For each truncation ratio the accuracy is exceptional for times less than the duration of the corresponding BIRF, i.e., $t \leqslant \alpha t_{eff}$; and (3) a truncation ratio $\alpha > 1.5$ produces errors less than 5%.

In view of the studies in both frequency and time domains it is concluded that a truncation ratio of $\alpha \geqslant 1.5$ yields acceptable accuracy for all practical applications.

8. Conclusions

The present work proposes a new BEM methodology for solving the wave propagation problem in 3D acoustic media in the DTD. The method is based on BIRF of the boundary of the domain and the associated B-spline fundamental solutions are introduced. Responses to arbitrary excitations are computed based on a simple superposition of the BIRF functions. In view of the methodological developments the following conclusions are made:

(1) The BIRF is a characteristic of the system is independent of the external excitation and needs to be computed only once for a specific geometry of the free surface of the solution domain.
(2) Because of the small, finite duration of the B-spline impulse excitation, and the wave attenuation, the number of time steps that the BIRF matrices are obtained for is considerably smaller than the time history of the response due to arbitrary excitations of long duration.
(3) The convergence of the proposed methodology does not depend on the selection of the time step as is the case with RP methods reported in the literature.

It is demonstrated that the proposed method is highly accurate and efficient.

References

[1] M. Bonnet, *Boundary Integral Equation Methods for Solids and Fluids*, Wiley, New York, 1995.
[2] K.M. Mitzner, Numerical solution for transient scattering from a hard surface–retarded potential technique, *Journal of the Acoustical Society of America* 42 (1967) 391–397.
[3] H. Huang, G.C. Everstine, W.F. Wang, Retarded potential techniques for the analysis of submerged structures impinged by weak shock waves, in: T. Belytschko, T.L. Geers (Eds.), *Computational Methods for Fluid–Structure Interaction Problems, AMD*, Vol. 26, ASME, New York, 1977, pp. 83–93.
[4] P.H.L. Groenenboom, Solution of the retarded potential problem and numerical stability, in: C.A. Brebbia (Ed.), *Boundary Element 6*, Springer, New York, 1984, pp. 4.57–4.74.
[5] A.M. Figueiredo, Differential-delay equations of advanced type and discretization of Kirchoffs integral equation, Ph.D. Thesis, Boston University, 1992.

[6] G.Y. Yu, S.T. Lie, S.C. Fan, Stable boundary element method/finite element method procedure for dynamic fluid–structure interaction, *Journal of Engineering Mechanics* 128 (2002) 909–915.
[7] D.C. Rizos, D.L. Karabalis, A time domain BEM for 3-D elastodynamic analysis using the B-Spline fundamental solutions, *Computational Mechanics* 22 (1998) 108–115.
[8] D.C. Rizos, K.G. Loya, Dynamic and seismic analysis of foundations based on free field B-Spline characteristic response histories, *Journal of Engineering Mechanics* 128 (2002) 438–448.
[9] D.C. Rizos, Z. Wang, Coupled BEM–FEM solutions for direct time domain soil–structure interaction analysis, *Engineering Analysis with Boundary Elements* 26 (2002) 877–888.
[10] D.C. Rizos, Advanced time domain Boundary Element Method for general 3-D elastodynamic problems, Ph.D. Thesis, University of South Carolina, 1993.
[11] L. Gaul, M. Wanger, W. Wenzel, N. Dumont, Numerical treatment of acoustic problems with the hybrid boundary element method, *International Journal of Solids and Structures* 38 (2001) 1871–1888.
[12] C.T. Dyka, R.P. Ingel, G.C. Kirby, Stabilizing the retarded potential method for transient fluid–structure interaction problems, *International Journal for Numerical Methods in Engineering* 40 (1997) 3767–3783.
[13] O. Czygan, O. von Estorff, Fluid–structure interaction by coupling BEM and nonlinear FEM, *Engineering Analysis with Boundary Elements* 26 (9) (2002) 773–779.